33RD CONGRESS
OF THE INTERNATIONAL COUNCIL
OF THE AERONAUTICAL SCIENCES
STOCKHOLM, SWEDEN, 4-9 SEPTEMBER, 2022

DYNAMIC STRESS SIMULATION AND ASYMMETRY STATOR DESIGN FOR A FAN BLISK

Yixiong Liu[1], Kening Xu[2], Yuzhi Chen[1], Yunwu Wu[1], Qing Du[1], Da Mo[1,*]

[1,*]AECC Shenyang Engine Research Institute, Shenyang 110015, China

[2]Aero Engine Academy of China, Beijing 10130, China

Abstract

The complex working load and complicated airfoils have called for precise estimation of dynamic for the fan blisk structure. This paper performs numerical simulation using the weak-coupling method to predict the real vibration stress of the fan blisk. The dangerous nodal diameter (ND) was identified considering the influences of upstream and downstream stators. Afterwards, the coupled Campbell diagram was presented to figure out the possible dangerous speed. Then, the three dimensional unsteady flow analysis were carried out and the generated pressure was interpolated to the blade surface within a time domain. The tested damping ratio for the first, second and third mode was 0.007, 0.003, 0.002 respectively. They were implemented in the dynamic stress prediction. The calculated dynamic stress was 35 MPa, which is consistent with the experimental value 33 MPa. Finally, the asymmetry stator design was studied and the dynamic stress shows a 12 MPa drop compared to the symmetry design. This finding has highlighted the importance of breaking the symmetry of the blisk and reduce the vibration stress.

Keywords: forced response, dynamic stress, vibration suppression, asymmetry stator, nodal diameter

1. Introduction

Nowadays, the increasing demand for high thrust-weight ratio has resulted in higher requirements in aerodynamic loading. Furthermore, the airfoils are becoming complex and sophisticated with thin and light materials, such as the blisk structure, composite material blade and hollow blade. It has brought a new challenge for the aeroengine blade vibration design. One of the main tasks of aero-engine blade vibration design is to ensure that harmful resonance does not occur within the working speed range. Typically, the Campbell diagram is utilized to assess the results of vibration characteristics and predict the resonance speed margin of the blade. However, the Campbell diagram cannot evaluate the real vibration stress and it is only applicable for preliminary vibration design. It is especially the case for the blisk structure, which might pose high cycle fatigue (HCF) risks. Unlike the conventional blade, the blisk structure features thin airfoil and strong blade-disc coupling effects. Consequently, the blade-disc coupling analysis should be carried out to ensure a reliable design. However, it is difficult to avoid all the resonance points and the most dangerous mode should be selected for the vibration response. Meanwhile, the blisk is tenon-free design and the damping is much lower than the blade-disc system. Combining the fact that the underplatform damper and shroud are not accessible to blisk structure, it is more vulnerable to HCF failure.

Recently, the fluid-solid coupling method has been implemented to analyze the vibration response of the blade, which proves to be promising methods for blade dynamic stress estimation. One of the well-established methods is the weak coupling method for vibration response simulation since the strong coupling approach is time-consuming. It ignores the influences of the aerodynamic force on the blade mode but provides a deeper insight into the vibration response prediction.

In order to obtain the real vibration stress of the blade and blisk, researchers around the world have carried out numerous investigation. Kielb [1] carried out numerical simulation and experimental verification of the forced response resulting from the wake excitation of upstream stator. Sayma [2] proposed a nonlinear vibration response prediction model. It is capable of reflecting the coupling effects of fluid and structure by moving fluid mesh according to the structural motion. Zhao [3] performed three-dimensional flow analysis and then carried out the harmonic response analysis using ANSYS software. Then the steady-state forced vibration response of the blade was obtained. Wang [4][5] interpolated the unsteady pressure calculation results into the blade surface and achieved the dynamic stress with the estimated damping ratio. The upstream stator wake was also considered during the simulation. Wang [6] used the fluid-solid coupling method to calculate the response of the wide-chord hollow fan blade and obtained the dynamic deformation of the blade. Zhang [7] perfected the two-way sequential coupling theory and calculated the response of the stator blade under air flow excitation. Gong [8] combined CFX and ANSYS software to predict the deformation and stress using a single passage coupling-model under steady loading. Zhang [9] also used the two software to undertake the numerical simulation of the full-cycle three-dimensional intake distortion of a compressor, taking into account the fluid-structure coupling effects. Xu [10][11] developed a three-dimensional turbine aeroelastic calculation software system to solve the transient deformation and dynamic stress of the blade based on the time marching method. The dynamic stress of a mistuned blisk was predicted and validated. Niu [12] studied the effects of non-uniform stator layout on the vibration response of rotor blades. Wang[13] utilized the analytical method and finite element method to consider the influences of different aerodynamic loading on the blade vibration response.

A systematic investigation was performed in order to estimate the dynamic stress of blisk structure. The modal analysis was carried out using the cyclic boundary conditions and the geometry nonlinearity was considered. Afterwards, the most dangerous nodal diameter was achieved by the empirical equations. The coupled Campbell diagram and the low-order resonance within the operating speed range were obtained. Meanwhile, the unsteady analysis was undertaken considering the downstream and upstream stators. The obtained unsteady pressure was interpolated to the blade nodes for transient response analysis. The dynamic stress was obtained using the tested and assumed damping ratio. Then, the asymmetry stator design was carried out to explore its potential in dynamic stress reduction. Finally, the numerical results were validated by the engine test.

2. Methodology

2.1 Investigation Case

A high-performance fan blisk was investigated in the paper. The material of the fan blisk is TC17 alloy with the density 4640kg/m^3 and elastic modulus 113.5GPa. The counts of the fan blisk, upstream stator and downstream stator are 20, 23 and 45 separately. As shown in Fig.1, a 1/20 finite element model was established for modal analysis with the hexahedral elements. The cyclic boundary was implemented with the maximum nodal diameter reaching 10. Also, the geometric nonlinearity was considered implementing the perturbation module.

Considering it might be time-consuming and low efficient by performing the fluid-structure strong coupling simulation, the coupling effects of the vibration and pressure were ignored.

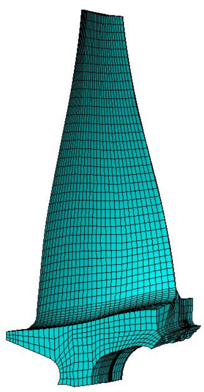

Figure 1 –Finite element model.

2.2 Dangerous Resonance Speed Identification

The first step of the dynamic stress estimation process is to identify the dangerous resonance speed. The dangerous ND was found out according to Eq.(1) [14-16]. It not only considers the condition that the ND equals to the excitation, but also includes the upstream and downstream stator excitation. Eq.(1) provides a comprehensive insight into the excitation calculation. Afterwards, the coupled Campbell is depicted, as shown in Fig.2. In this scenario, only the frequency ranging from first to ten modes are presented. Afterwards, the dangerous resonance speed was obtained by sorting the frequency safety margin.

$$d_m = |kN_s - nN_R| \tag{1}$$

Where:

d_m is the dangerous nodal diameter;

k is the engine excitation;

N_s is the upstream or downstream stator number;

n is integer;

N_R is the blisk number。

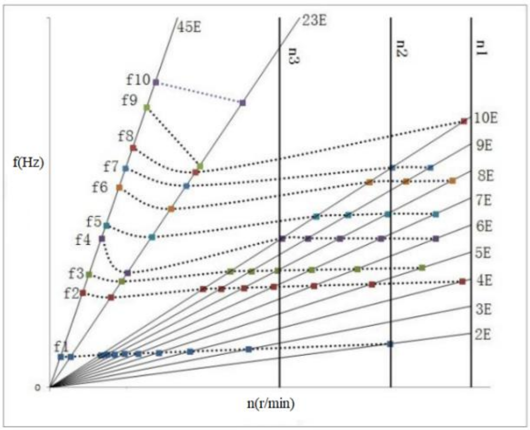

Figure 2–Coupled Campbell diagram

2.3 Damping ratio

Damping ratio is key factor affecting the vibration response of the fan blisk since it decides how much energy is consumed during vibration. In this scenario, the free attenuation method (FAM) was utilized to achieve the damping ratio of the fan blisk. A force hammer was implemented to trigger the vibration with many strain gauges mounted on the blisk.

The specific equation for damping calculation is shown in Eq.(2), it considers the involved peak response of the related frequencies.

$$\zeta = \frac{\ln \dfrac{A_1}{A_{i+1}}}{\sqrt{4\pi^2 i^2 + (\ln \dfrac{A_1}{A_{i+1}})^2}} \tag{2}$$

Where:

d_m is the dangerous nodal diameter;

k is the engine excitation;

N_s is the upstream or downstream stator number;

n is integer;

N_R is the blisk number。

During data analysis, the measured signals with multi-order frequencies are separated into single-frequency vibration signals of each target order frequency by digital bandpass filtering. Afterwards, the time-domain damping ratio is calculated to obtain the corresponding damping ratio of each mode vibration frequency. Through the peak-picking method, the frequency response function is divided into the real part and the imaginary part. The modal parameters are obtained by reading the data directly from the real and virtual frequency diagrams.

2.4 Unsteady analysis

On the basis of the resonance speed obtained, the CFX software was utilized to analyze the three-dimensional unsteady dynamic pressure. Taking the first bending mode resonance excited by 2 engine order (EO) as an example, the single-passage steady analysis of all rows was carried out. The boundary conditions of inlet and outlet were extracted and expanded to cater to the unsteady analysis. It should be noted that a 1.5-stage whole-passage model was established consisting of the upstream stator, blade and downstream stator, as shown in Fig.3. Both the upstream wake and downstream potential flow were taken into consideration, which could provide precise dynamic pressure for blade. The total nodes of the model is 30 million and the k-ε turbulence model was employed. The standard wall boundary was used. In the unsteady calculation, the transient module was selected, and the time step was defined as 1/40 of blade passing time. This is to ensure that the interactions between the blade and stator was fully considered.

It should be noted that the 2EO to 6EO excitation was also considered using the harmonic index method. The static pressure of the blade surface converged after several oscillation cycles was used for dynamic stress prediction.

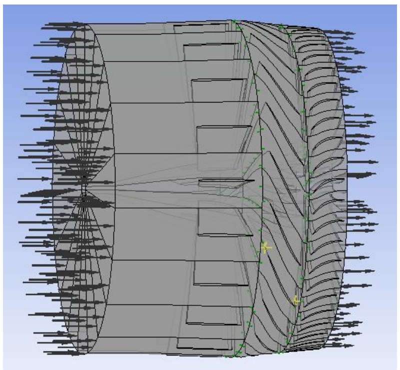

Figure 3–1.5 stage fluid model

2.5 Dynamic Stress Calculation

In this scenario, the dynamic stress is obtained using the in-house software DasRotor. It extracts the CFD grids from the unsteady simulation and convert the hot blade profile to cold airfoil for finite element model. Then, the dynamic pressure is interpolated into the blade surface in the time domain. Finally, the dynamic stress of the blisk is obtained by the transient analysis with the tested damping ratio.

3. Results Analysis

3.1 Dangerous Resonance Speed

As indicated previously, the counts of the upstream stator NS1, blade NR and downstream stator NS2 are 23, 20 and 45 respectively. According to Eq.(1), the dangerous ND that might pose resonance risk are 3 and 5, as presented in Table 1. It worth mentioning that the calculated ND larger than 10 is quit since the maximum available ND is 10.

Table 1 Dangerous ND related to stators

n	N_{S1}	N_R	ND	N_{S2}	ND
1	23	20	**3**	45	25
2	23	20	17	45	**5**
3	23	20	37	45	15

Table 2 Resonance speed results

k/dm	Mode	Resonance speed/（r/min）	Frequency/Hz
2E/2ND	1	9007	293
4E/4ND	2	10764	718
5E/5ND	2	8400	700
6E/6ND	3	8020	802

The relative von-mises stress distribution of the first bending mode at 2ND is presented in Fig.4. There are two distinct petal-like sections representing the blade vibration under 2ND. It mainly results from the strong stiffness of the disc and the blade vibration has to spread around the circumferential direction.

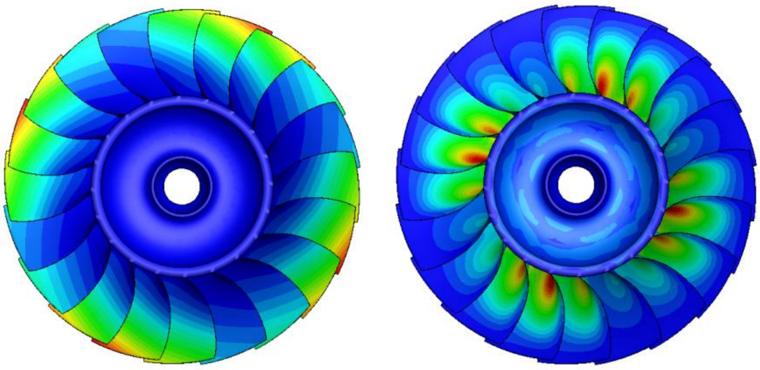

Figure 4–Relative von-mises stress distribution of the first bending mode at 2ND

3.2 Damping ratio

Considering the system errors, force impacts and influences of strain gauges, three blades were randomly selected in the circumferential direction to paste strain gauges at the same part of the tip with the hammer connected to the sensors. The test results were repeated three times under the same loading, and the average modal damping ratio was used for dynamic stress estimation.

The average values of the first to three mode frequencies and the corresponding modal damping ratio are obtained, as shown in Table 3. An apparent trend is that the modal damping ratio drops significantly with the increase of frequency, indicating that the higher mode might provide little damping. For the high-order mode damping ratio, it was given according to reference [17].

Table 3 Frequency and damping ratio

Items	1st	2nd	3rd
Frequency/Hz	200	627	755
Damping ratio	0.007	0.003	0.002

3.3 Dynamic Stress Estimation and Validation

By performing the unsteady simulation of the fan blisk, the static pressure of the blade surface was obtained after several ocilication cycles, as shown in Fig.5. After that, the pressure is interpolated into the finite element model for vibration response prediction.

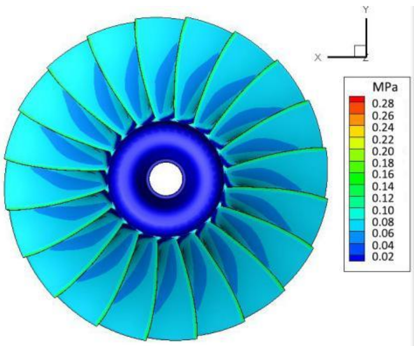

Figure5-Static pressure distribution after convergence

The static analysis was first carried out using the perturb module and the new balance position of the blisk was obtained under centrifugal loading. Then, the transient response analysis was performed including the prestress effects. The unsteady aerodynamic loading on the blade surface obtained from Fig.5 was interpolated into the finite element model as the nodal pressure on the blade surface. At the same time, the modal damping ratios are given in the form of Rayleigh damping according to the experimental data obtained in Table 3. During the simulation, the maximum relative stress point A was selected as the monitoring point, as demonstrated in Fig.6. After several iterations, the vibration stress of the monitoring point on the blade surface tends to converge, as depicted in Fig.7. At this time, the calculated vibration stress is the real vibration stress of the blade disk, and the vibration stress at point A after stabilization is about 35MPa. The detailed stress distribution of each blade is depicted in Fig.8. Obviously, the maximum dynamic stress still locates in the blade root sections.

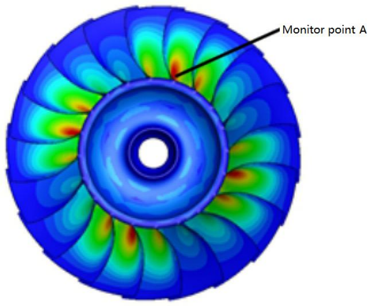

Figure6-Dynamic stress monitor point

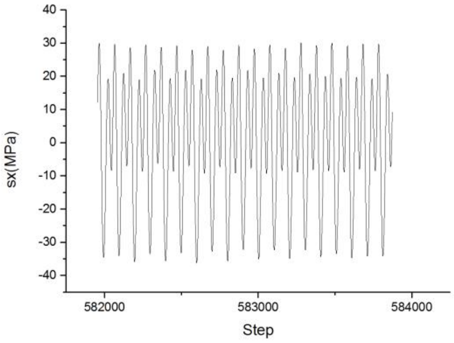

Figure7-Dynamic stress curve for first bending mode

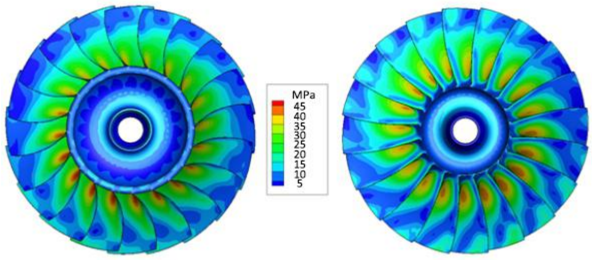

a) Suction side   b) Pressure side

Figure8-Dynamic stress distribution for first bending mode

In order to validate the numerical simulation results, a verification experiment was carried out. The strain gauges were mounted on the blade surface, as shown in Fig.9. The positions of the strain gauges are normalized values. By performing the engine test, the real vibration stress of the blade was achieved and compared with the simulation results in Table 4.

What is interesting is that the dynamic stress prediction are accurate for the low-order mode. For example, the predicted stress and tested stress for A was 35MPa and 33 MPa respectively, which are very close. It is the same for point B. However, the stress for high-order mode exists certain errors. For the C position, the calculated stress and the real stress was 7 MPa and 12 MPa with the error reaching 41.7%. Point D also employs 30.6% errors of the stress prediction. Nevertheless, the calculated frequency for all the points were consistent with the test. Considering that the size, shape and material properties of the blade disk in the reference are different from those studied in this paper, as well as the influence of mistune and other factors, there is a certain error in the given high-order damping ratio. Comprehensive analysis shows that the main reason for the error in the prediction of high-order vibration stress is the slight deviation between the selected damping ratio and the real condition.

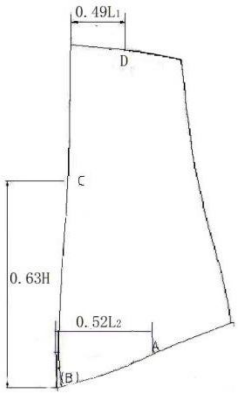

Figure9-Strain gauges mounted on the blade

Table 4 Results comparisons of simulation and test

Position	A	B	C	D
Maximum tested stress/MPa	33	10	12	36
Maximum calculated stress/MPa	35	9	7	25
Tested frequency/Hz	290	290	6850	5608
Calculated frequency/Hz	293	293	6870	5606

3.4 Asymmetry Stator Design

Asymmetry stator design is an effective measure for blade vibration suppression since it weakens the wake or potential flow of the stator. Consequently, the stator excitation would be changed and the blade resonance is shifted and relived. In this paper, the upstream stator was designed to be asymmetry in circumferential direction to observe its influences on the blisk stress. As shown in Fig.10, the upper side has 11 stators while the lower side has 12 stators, which is different from the uniformly distributed 23 stators. The same process was performed to obtain the dynamic stress of the blisk after the asymmetry stator adjustment. The dynamic stress comparison is presented in Fig.11. Obviously, the dynamic stress of the below half of the suction side of the blisk has significantly dropped 12 MPa, reaching 36% of the original tested stress. It could be concluded that the asymmetry stator could be implemented to curb the dynamic stress of the fan blisk for engineering practice.

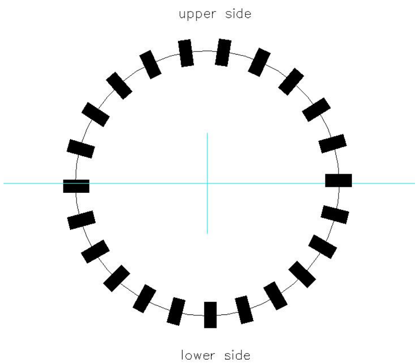

Figure10-Asymmetry stator design

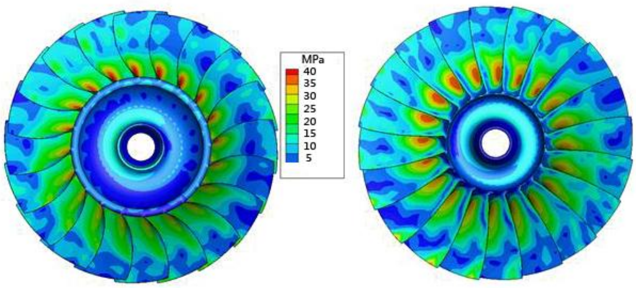

a) Suction side b) Pressure side

Figure11-Dynamic stress results of the blade with asymmetry stator design

4. Conclusions

In this paper, the numerical simulation and experimental validation of the dynamic stress of the fan blisk are carried out. Meanwhile, the asymmetry stator design was investigated. The main outcomes are listed as below:

(1) The calculated dynamic stress of point A and point B are close to the tested values while the high-order mode stress are lower than the real stress, resulting from the damping ratio. This finding has highlighted the importance of incorporating accurate modal damping ratio for dynamic stress prediction.

(2) The simulation process provides a better understanding in dynamic stress estimation using the weak-coupling method. It is necessary to establish a 1.5-stage whole-circle fluid model to achieve precise dynamic pressure.

(3) The asymmetry stator design has offered 12 MPa drop in dynamic stress while the fan performance is not affected. It provides a good measure for vibration suppression for blisk structure since the common damper are not accessible.

5. Contact Author Email Address

Da Mo: dada1204@126.com

6. Copyright Statement

Acknowledgement

The authors would like to thank AECC Shenyang Engine Research Institute for the support and fund.

References

[1] Kielb J J, Abhari R S, Dunn M G. Experimental and Numerical Study of Forced Response in a Full-scaled Rotating Turbine. ASME 2001-GT-0263,200.

[2] Sayma A I, Vahdati M, Imregun M. An Integrated Nonlinear Approach for Turbomachinery Forced Response Prediction. Part I: Formulation. Journal of Fluid and Structures, 2000, 14(1):87-101.

[3] Zhao Shujun. Investigation on Three-Dimensional unsteady Flow Calculation and Foreced response. Xi' an:, Northwestern Polytechnical University,2003. (in Chinese)

[4] Wang Mei. Solving the Problems of Transforming Unsteady Flow Analysis Results to Load Pressure Field.Gas Turbine Experiment and Research, 2005, 18(3):15-18. (in Chinese)

[5] Wang Mei, Jiang Hefu, Lv Wenlin. Method to Predict the Blade Vibration Stress Induced by Wake Flow. Journal of Aerospace Power, 2007, 22(4):608-613. (in Chinese)

[6] Wang Ying, Tao Zhi, Fu farong, et al. Response Analysis of Fluid and Solid Coupling Characteristics for a Wide-chord Hollow Fan Blade. Journal of Aerospace Power, 2008, 23(12):2177-2183. (in Chinese)

[7] Zhang Dayi, Ma Yanhong, Hong Jie, et al. Dynamical Response Analysis on Blades Arisen by Aerodynamic Forces Through Sequential Mehtod. Journal of Aerospace Power, 2009,24(7):1523-1529. (in Chinese)

[8] Gong Sanwei, Ren Liyun, Liu Huoxing, et al. Fluid-solid Interaction of Rotor Blade in Last Stage of Steam Turbine. Thermal turbine, 2007,36(3):153-167. (in Chinese)

[9] Zhang Mingming, Hou Anping, Wang Qiang. Numerical Investigation of Blade Vibration Response Induced by Inlet Distortion in Axial Compressor. Journal of Propulsion Technology, 2011,32(4):466-470. (in Chinese)

[10]Xu Kening, Wang Yanrong. Numerical Simulation of Aeroelastic Response in Compressor Rotor Blades[J]. Journal of Aerospace Power, 2010,25(10):2207-2210. (in Chinese)

[11]Xu Kening, Wang Yanrong,Liu Jinlong. Vibration Response Analysis on Mistuned Blaede Disk Assembly of Compressor Rotors. Gas Turbine Experiment and Research, 26(3):6-11. (in Chinese)

[12]Niu Yonghong, Hou Anping, Zhang Mingming,et al. Effects of Asymmetric Vane Spacing on Rotor Blade Vibration. Journal of Propulsion Technology, 2015,36(7):1079-1084. (in Chinese)

[13]Wang Jiao. Investigation on the vibration characteristics and response anslysis method.Shenyang: Northeastern University,2010. (in Chinese)

[14]Wang Yanrong, Tian Aimei. Several Issues in the Implementation of Vibration Analysis of Bladed Disk. Journal of Propulsion Technology, 2002，23(3):234-236. (in Chinese)

[15]Yao Jianyao. Forced Response Analysis of Bladed Disk under Fluid Excitation. Beijing University of Aeronautics and Astronautics,2010.(in Chinese)

[16]Qi Zheng, Wang Jianjun. Excitation Order Verification of Bladed-disk Coupled Resonance Condition. Journal of Beijing University of Aeronautics and Astronautics,2014,40(7):984-987. (in Chinese)

[17]Srinivasan A V. Flutter and Resonant Vibration Characteristics of Engine Blades. Journal of Engineering for Gas Turbines and Power, 1997, 119(4):742-775.